Human Molecular Genetics, 2014, Vol. 23, No. 2 **502–513**
doi:10.1093/hmg/ddt444
Advance Access published on September 10, 2013

BSCL2/seipin regulates adipogenesis through actin cytoskeleton remodelling

Wulin Yang[1], Shermaine Thein[1], Xiaorui Wang[1], Xuezhi Bi[1], Russell E. Ericksen[1], Feng Xu[2] and Weiping Han[1,2,3,4,5,*]

[1]Singapore Bioimaging Consortium, [2]Singapore Institute for Clinical Sciences and [3]Institute of Molecular and Cell Biology, Agency for Science, Technology and Research (A*STAR), Singapore, Singapore, [4]Duke-NUS Graduate Medical School, Singapore 169857, Singapore and [5]Department of Biochemistry, Yong Loo Lin School of Medicine, National University of Singapore, Singapore 117597, Singapore

Received July 6, 2013; Revised August 16, 2013; Accepted September 5, 2013

Seipin regulates lipid homeostasis by preventing lipid droplet (LD) formation in non-adipocytes but promoting it in developing adipocytes. Here, we report that seipin interacts with 14-3-3β through its N- and C-termini. Expression of 14-3-3β is upregulated during adipogenesis, and its deletion results in defective adipogenesis without affecting key adipogenic transcription factors. We further identified the actin-severing protein cofilin-1 as an interacting partner to 14-3-3β. Cofilin-1 was spatiotemporally recruited by 14-3-3β in the cytoplasm during adipocyte differentiation. Extensive actin cytoskeleton remodelling, from stress fibres to cortical structures, was apparent during adipogenesis, but not under lipogenic conditions, indicating that actin cytoskeleton remodelling is only required for adipocyte development. Similar to seipin and 14-3-3β, cofilin-1 knockdown led to impaired adipocyte development. At the cellular level, differentiated cells with knockdown of cofilin-1, 14-3-3β or seipin continued to maintain relatively intact stress fibres, in contrast to cortical actin structure in control cells. Finally, 3T3-L1 cells expressing a severing-resistant actin mutant exhibited impaired adipogenesis. We propose that seipin regulates adipogenesis by recruiting cofilin-1 to remodel actin cytoskeleton through the 14-3-3β protein.

INTRODUCTION

Obesity, now a pandemic, contributes to the development of diabetes and other metabolic diseases. At the other extreme, lipodystrophy is also associated with severe insulin resistance and diabetes. There are four major types of congenital lipodystrophy. Type 2 is the most severe (CGL2) and is caused by homozygous loss-of-function mutations of *BSCL2* gene, which encodes the seipin protein (1). Mouse genetic studies have confirmed the causal relationship of seipin and lipodystrophy (2,3) by showing altered adipocyte development and lipolysis in seipin knockout mice. However, the underlying molecular mechanisms remain unclear.

The secondary structure of seipin in all studied species is quite similar, including a conserved central core domain, and diverse cytosolic N- and C-termini (4,5). Previously, we demonstrated that mammalian seipin contains at least two functional domains, a conserved core sequence including two transmembrane domains with an ER luminal loop, and an evolutionarily acquired C-terminus (4). Except for a few point mutations, most of the lipodystrophy-associated *BSCL2* mutations are missense mutations that result in C-terminally truncated proteins due to early transcription termination (1,6,7). Some of the truncated proteins retain the conserved core sequence, such as R275X and Q391X (1,6,7), but still lead to lipodystrophy, indicating that the evolutionarily acquired C-terminus confers seipin new functions that are important in regulating adipogenesis.

Although it is critical for adipogenesis, seipin inhibits LD production and accumulation in preadipocytes and other nonadipocyte lineages through its conserved core sequence (4). On the other hand, the mammalian seipin C-terminus, acquired during the ectothermic to endothermic transition, regulates lipid homeostasis by promoting adipogenesis to accommodate storage of excess nutrients in the form of lipids (4) and to provide heat insulation. The cell-autonomous function model

*To whom correspondence should be addressed. Email: weiping_han@sbic.a-star.edu.sg

is consistent with findings from yeast to human studies. For example, CGL2 patients and seipin-deficient mice lack fat tissue, but display accumulation of fat in liver and muscles.

To dissect the molecular mechanisms underlying the function of seipin in regulating adipogenesis, we performed mass spectrometry to identify novel proteins that interact with seipin. We report that seipin interacts with 14-3-3β in the cytoplasm, which in turn binds to the actin-severing protein cofilin-1 under insulin stimulation. Based on the current study and previous findings from our laboratory and others, we propose that actin cytoskeleton remodelling is central to the formation of mature adipocytes, and that seipin regulates this process by recruiting cofilin-1 through its interacting partner 14-3-3β.

RESULTS

Seipin interaction with 14-3-3β

Both *in vivo* and *in vitro* findings have indicated that the lipodystrophy-associated protein seipin plays an important role in adipogenesis, but the molecular mechanism involved is largely unknown (2,3,8,9). In our previous work (4), we found that seipin regulates lipid homeostasis through its two distinct functional domains, the core sequence generally controls LD accumulation in non-adipocytes, preventing lipid overloading that may lead to lipotoxicity. Consistent with this model, compared with control cells (Ctrl.), overexpression of seipin (WT) or its core sequence (ΔCT) strongly inhibited oleate-induced LD production and accumulation in preadipocytes incubated with Bodipy FL C16 for 18 h (Fig. 1A). Conversely, seipin appeared to be essential for LD accumulation during adipogenesis (2,3), which is likely attributable to actions mediated by the C-terminus (4). To understand how seipin regulates the cellular processes during adipogenesis and discovery of its interaction partners, we used a GST-fused seipin C-terminus to pull down proteins from adipose tissue lysate, and identified the scaffold protein 14-3-3β as a putative binding partner (Fig. 1B and Supplementary Material, Fig. S1). Co-IP experiments in 293 T cells were used to confirm the interaction of seipin and 14-3-3β (Fig. 1C and D). To determine the sequence of seipin required for its binding to 14-3-3β, we coexpressed Flag-tagged 14-3-3β and seipin truncation mutants (10) for Co-IP experiments (Supplementary Material, Fig. S2). Deletion of cytosolic N- or C-terminus of seipin dramatically decreased its binding with 14-3-3β (Fig. 1E). Interestingly, deletion of the loop region of seipin appeared to result in its stronger binding affinity to 14-3-3β. These results indicate that the cytosolic N- and C-termini of seipin may cooperate to bind 14-3-3β. To confirm their interaction in adipocytes, we expressed myc-tagged seipin in 3T3-L1 cells and cultured the cells in the adipocyte differentiating medium for 8 days. Seipin pulled down 14-3-3β in preadipocytes, and all subsequent stages of adipocyte differentation to a similar extent (Fig. 1F). Moreover, the seipin and 14-3-3β interaction was not altered by insulin or isoproterenol stimulation (Fig. 1F), suggesting a constitutive association between the two proteins. Taken together, these results show that seipin interacts with 14-3-3β through its cytosolic N- and C-termini in a constitutive manner.

Reduced LD accumulation and lipid levels in 14-3-3β KD cells

The 14-3-3 family is a group of scaffolding proteins, which play a multitude of roles in diverse cellular processes through its signalling transduction capacity. Therefore, we hypothesize that 14-3-3β may transduce seipin-governed lipid storage signalling to the cytoplasm, where it regulates pathways to store excessive lipids. We first examined the expression of 14-3-3β at different stages of adipogenesis. At Day 0, 14-3-3β expression was nearly undetectable, but significantly increased after adipogenic induction (Day 2) (Fig. 2A). The expression levels were highest at terminal stages of differentiation, i.e. on Day 8 and beyond. A similar expression pattern was observed by using a real-time PCR, where mRNA levels tightly correlated with protein levels (Fig. 2B). To understand the role of 14-3-3β in adipogenesis, we generated loss-of-function mutants. Several shRNAs targeting murine 14-3-3β were subcloned into lentiviral vectors, and packaged viruses were used to infect 3T3-L1 cells. Two shRNAs (1433-KD1 and 1433-KD2) were selected based on their ability to decrease 14-3-3β mRNA and protein levels (Fig. 2C and D). Cells harbouring either of these two shRNAs were treated with an adipocyte differentiating cocktail. Both shRNAs significantly delayed lipid accumulation and reduced the total lipid content during adipocyte differentiation when compared with control cells on Days 5 and 8 (Fig. 2E and F). To determine what processes were affected in 14-3-3β KD cells, we measured transcription factors critical in the regulation of adipogenesis, along with adipogentic markers by a real-time PCR (Fig. 2G and H). As expected, adipogenic markers, such as *Glut4* and *LDLR*, were significantly reduced in KD cells, consistent with defective adipogenesis. Surprisingly, adipogenic transcription factors, such as master regulators *PPARγ, C/EBPα*, and initiation factors, *C/EBPβ, C/EBPσ* and *Srebp1c*, were not affected by the 14-3-3β KD (Fig. 2G and H), suggesting that 14-3-3β does not directly regulate the transcription factor network in the adipogenesis process. We also determined the colocalization pattern of seipin and 14-3-3β during adipogenesis. At all the stages of differentiation, seipin colocalized with 14-3-3β to a similar extent (Supplementary Material, Fig. S3). Together, these data suggest that 14-3-3β functions as a relay station and scaffold to bring together additional interacting partners and regulators of the adipogenic process.

14-3-3β Interaction with cofilin-1 during adipocyte development

To identify interacting partners to 14-3-3β that may be involved in the control of lipid storage and adipocyte development, we performed pull-down experiments with GST-14-3-3β in adipocytes followed by mass spectrometry analysis. Under insulin stimulation, an actin-severing protein cofilin-1 was found to bind 14-3-3β (Fig. 3A and Supplementary Material, Fig. S4), and the insulin-stimulated binding was confirmed by coimmunoprecipitation of endogenous 14-3-3β and cofilin-1 (Fig. 3B). Serine-24 of cofilin-1 lies within a prototypical 14-3-3 recognition motif RSXpSP (11), so we tested whether this site was involved in the binding of 14-3-3β and cofilin-1. Immunoprecipitation studies indicated that the phosphomimetic mutant S24D

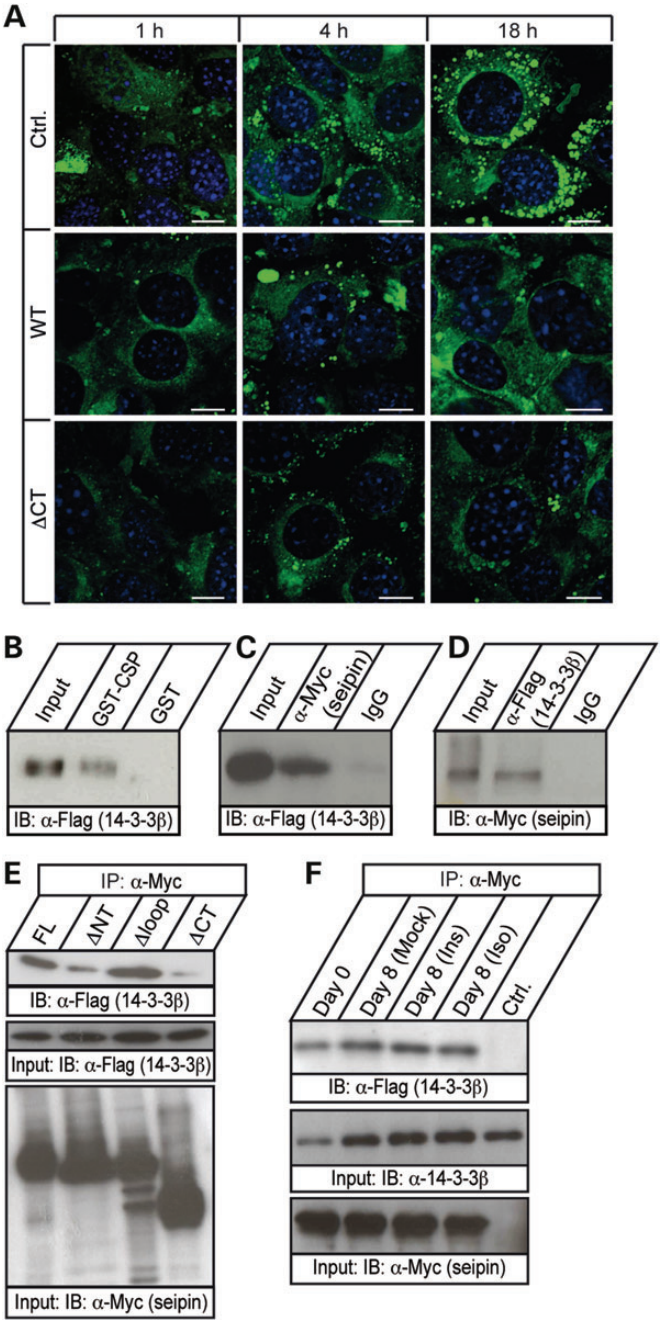

Figure 1. Seipin associates with 14-3-3β protein through its N- and C-termini. (**A**) Bodipy staining of nascent LDs in different groups of 3T3-L1 cells expressing wild-type seipin (WT-Seipin), C-terminus truncated seipin (ΔC-Seipin) or empty vector (Ctrl.), and visualized under a confocal microscope. Scale bars = 10 μm. (**B**) GST pull-down assay using a GST-fused C-terminus of seipin (GST-CSP) to pull down binding partners from fat tissue lysate, compared with the control group with GST protein (GST). (**C** and **D**) 293T cells were co-transfected with Myc-tagged seipin and Flag-tagged 14-3-3β. Two days after transfection, the cells were lysed in lysis buffer. Cell lysate was incubated with control IgG or anti-Myc (C), IgG or anti-Flag (D). Immunoblot (IB) using antibodies against either Flag (C) or Myc (D) revealed a seipin-14-3-3β interaction. (**E**) 293T cells were co-transfected with Flag-tagged 14-3-3β and Seipin-WT (FL) or seipin truncated mutants with deletion of the cytosolic N-terminus (ΔNT), the luminal loop (Δloop) or the cytosolic C-terminus (ΔCT). Two days after transfection, the cells were lysed in lysis buffer. Cell lysate was incubated with control IgG or anti-Myc antibody. IB using a Flag antibody revealed that 14-3-3β has different binding affinity to the various seipin mutants. (**F**) To further evaluate the interaction of seipin with 14-3-3β, immunoprecipitation was performed in 3T3-L1 cells. 3T3-L1 cells overexpressing myc-tagged seipin was induced to differentiate for 8 days, treated with insulin (Ins), isoproterenol (Iso) or left untreated (Mock). Cell lysates were incubated with an anti-Myc antibody. IB using an α-Flag antibody revealed that 14-3-3β bound to seipin under various conditions.

preferentially bound 14-3-3β compared with the phosphoinactive mutant S24A (Fig. 3C), suggesting that phosphorylation of serine 24 is important for its binding to 14-3-3β. We then examined the co-localization of these proteins at different stages of adipocyte differentiation. In pre-adipocytes (Day 0), a low degree of overlap was seen between 14-3-3β and cofilin-1. At this time point, cofilin-1 was concentrated in the nucleus, while 14-3-3β localized to the cytoplasm. The overlap of these two proteins significantly increased at Days 3 and 6 after adipogenic stimulation (Fig. 3D and E), largely due to the translocation of cofilin-1 from the nucleus to the cytoplasm. The finding of increased 14-3-3β and cofilin-1 interaction under insulin stimulation suggests a potential functional role of cofilin-1 in adipocyte development.

Actin cytoskeletal remodelling by cofilin-1 during adipogenesis

As cofilin-1 is an actin-severing protein, we examined the dynamics of actin cytoskeleton during adipocyte differentiation by staining the actin with rhodamine-labelled phalloidin. In undifferentiated pre-adipocytes (Day 0), actin filaments were well organized as regular stress fibres across the cell body (Fig. 4A). At Day 3 of adipogenic differentiation, actin filaments appeared to be disrupted from the center region of cell body (Fig. 4A), especially in regions where LDs were forming. As the cells further matured (Day 5 and Day 8), actin filaments were largely absent in the center cell body and organized only as peripheral cortical structures (Fig. 4A). LD development and accumulation were highly related to actin cytoskeleton dynamics, consistent with the notion that the actin network may be actively remodelled to control LD formation (Fig. 4A and Supplementary Material, Movie SA1–SA4). As a comparison, we examined actin cytoskeleton dynamics during oleate-induced LD production (lipogenesis), and found no evidence of actin cytoskeleton remodelling (Fig. 4B), i.e. the actin stress fibres maintained a regular array shape. It is worth noting that many smaller LDs accumulated in the cells after prolonged incubation with oleic acid (OA), suggesting that actin cytoskeleton is involved in the regulation of LD fusion and expansion, a critical step during adipocyte development (Fig. 4B and Supplementary Material, Movie SB1–SB4). To further test whether actin remodelling actively promotes adipogenesis, we treated 3T3-L1 cells with Latrunculin B (LatB) to promote actin cytoskeleton remodelling. At Day 7 after adipogenic cocktail treatment, lipid accumulation (Supplementary Material, Fig. S5A) and total lipid content (Supplementary Material, Fig. S5B) were increased under LatB treatment, consistent with a previous report showing that disassembly of the cytoskeleton promotes adipogenesis in ES cells (12). Together, these findings demonstrate extensive actin cytoskeleton remodelling during adipocyte development, a process that may be regulated by the actin-severing protein cofilin-1.

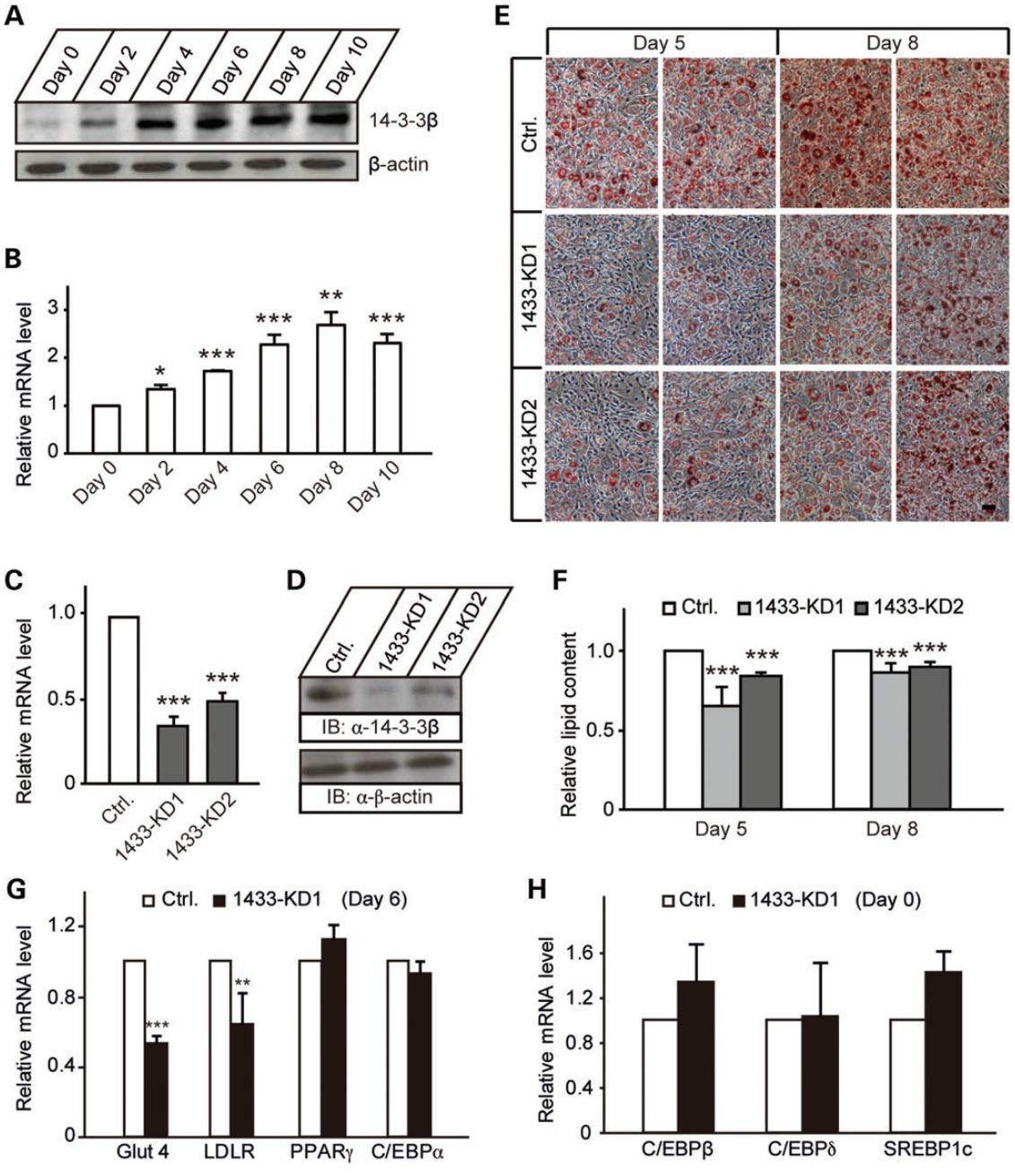

Figure 2. Knockdown of 14-3-3β prevents lipid accumulation during adipogenesis. (**A** and **B**) Expression levels of 14-3-3β were assessed by immunoblotting (A) and qPCR (B) at various time points during adipocyte differentiation. Data are presented as mean ± SD. $N = 3$ independent experiments, each measured in triplicates. (**C**) Two stable cell lines (1433-KD1 and 1433-KD2) with efficient downregulation of 14-3-3β when compared with the control group (Ctrl., scrambled siRNA) were selected based on the mRNA levels by qPCR (C) or protein levels (**D**). (**E**) Stable 14-3-3β (1433-KD1 and 1433-KD2) knockdown 3T3-L1 cells were stained with oil-red O at Days 5 and 8 after adipogenic cocktail treatment and assessed by microscopy (20×). Two representative fields are shown for each group. Scale bars = 50 μm. (**F**) Isopropanol extracts of oil-red O were used to assess relative total lipid content in 14-3-3β KD cells at Days 5 and 8 post adipogenic cocktail treatment. Data are presented as mean ± SD. $N = 3$-4 independent experiments. (**G**) Expression levels of adipocyte markers, GLUT4, LDLR and two master adipogenic regulators, PPARγ and C/EBPα, were determined by qPCR in stable KD cells (1433-KD) in comparison with the control group (Ctrl., scrambled siRNA) at Day 6. (**H**) Expression levels of adipogenic initiation regulators, C/EBPβ, C/EBPσ and Srebp1c, were determined by qPCR in stable KD cells in comparison with control cells (Ctrl., scrambled siRNA) at Day 0. Data are presented as mean ± SD. $N = 3$ independent experiments, each measured in triplicates. $^{*}P < 0.05$ and $^{**}P < 0.01$ versus. control cells.

Impaired actin cytoskeleton remodelling and adipogenesis in cofilin-1-deficient cells

To investigate the involvement of cofilin-1 in adipocyte development, we first examined the expression of cofilin-1 at different stages of adipogenesis. At Day 0, cofilin-1 expression was low, but increased significantly by Days 2 and 4 after adipogenic induction (Fig. 5A). A real-time PCR confirmed the expression pattern of *cofilin-1* during adipogenesis at the mRNA level

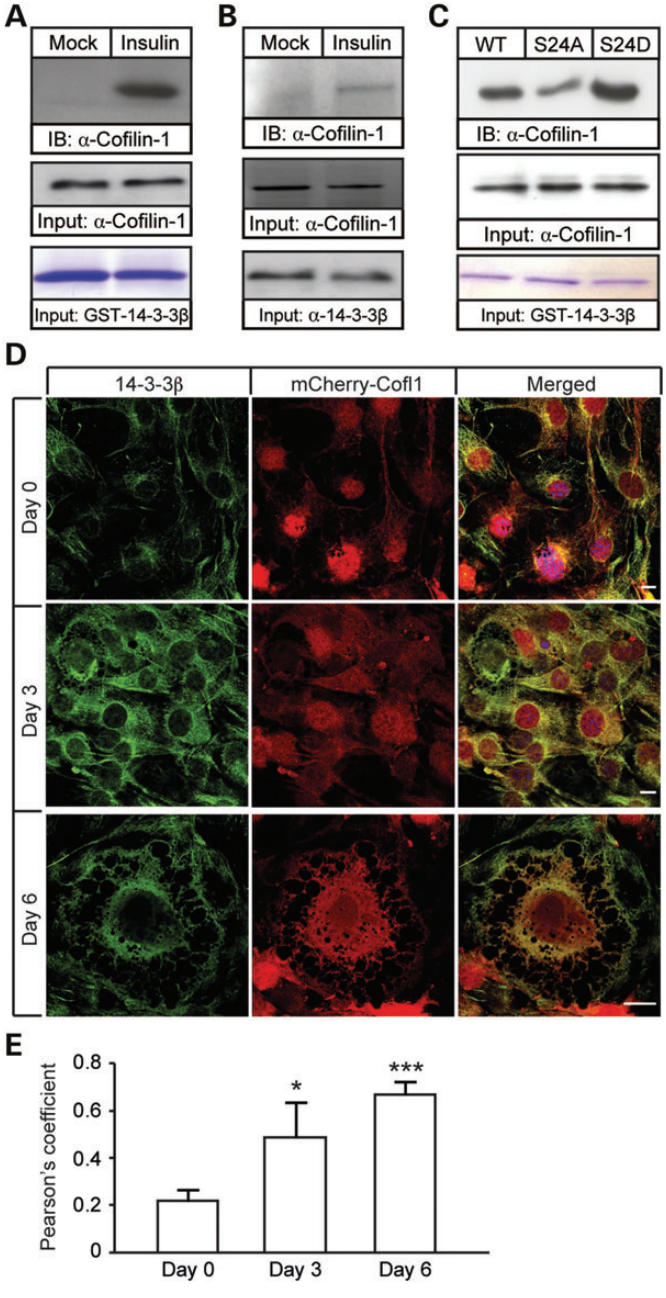

Figure 3. 14-3-3β interacts with the actin-severing protein cofilin-1 under insulin stimulation and mediates the localization of cofilin-1 during adipogenesis. (**A**) GST pull-down assay was performed by using GST-fused 14-3-3β (GST-1433) to pull down binding partners from differentiated 3T3-L1 cells under conditions with (Ins) or without (Mock) insulin stimulation. The input levels of confilin-1 and GST-14-3-3β were shown as detected by anti-cofilin-1 antibody or commassie blue staining, respectively. (**B**) Endogenous association of cofilin-1 and 14-3-3β was verified by co-IP with a 14-3-3β antibody under insulin treatment. The input levels of cofilin-1and 14-3-3β were shown as detected by anti-cofilin-1 antibody or anti-14-3-3β antibody, respectively. (**C**) GST pull-down assay in cells expressing WT, phosphomimetic or phosphoablative mutants of cofilin-1. The input levels of confilin-1 and GST-14-3-3β were shown as detected by anti-cofilin-1 antibody or commassie blue staining, respectively. (**D**) 3T3-L1 cells expressing mCherry-tagged cofilin-1 were fixed, stained with an anti-14-3-3β antibody at Days 0, 3 and 6 after adipogenic cocktail treatment, and imaged on a confocal microscope. Scale bars = 10 μm. (**E**) Pearson's coefficients for 14-3-3 and cofilin-1 colocalization were calculated by software bundled with a Nikon confocal microscope at the indicated time points. Data are presented as mean ± SD. $N = 3–4$ independent experiments.

(Fig. 5B). To examine the function of cofilin-1 in adipogenesis, we generated loss-of-function mutants. Several shRNAs targeting the murine *cofilin-1* were subcloned into lentiviral-based vectors and packaged viruses were used to infect 3T3-L1 cells. Two shRNAs (Cofl-KD1 and Cofl-KD2) significantly decreased the expression of cofilin-1 at both the mRNA and protein levels (Fig. 5C and D). Compared with control cells, KD of cofilin-1 significantly decreased lipid accumulation and total lipid content during adipocyte differentiation (Fig. 5E and F). As expected, adipocyte markers, such as Glut4 and LDLR, were significantly decreased in KD cells compared with controls (Fig. 5G). However, mRNA levels of adipogenic master transcription factors *PPARγ* and *C/EBPα*, and initiation factors *C/EBPβ, C/EBPσ* and *Srebp1c*, were similar between control and KD cells (Fig. 5G and H). These results support a functional role of cofilin-1 in regulating lipid accumulation and adipocyte development without directly modulating the adipogenic transcriptional cascade.

To determine whether cofilin-1 contributes to adipocyte development by regulating actin cytoskeleton remodelling during adipogenesis, we examined the actin cytoskeleton dynamics by using rhodamine-labelled phalloidin in adipocytes after 5 days of adipogenic cocktail treatment. At this time point, the actin cytoskeleton of control cells was localized to the cortical region near the plasma membrane. In contrast, a relatively intact actin fibre network was found in the cell body of confilin-1 KD cells (Fig. 6A). A similarly intact actin cytoskeleton pattern was observed in 14-3-3β KD cells (Fig. 6B) and seipin KD cells (Supplementary Material, Fig. S6). As the morphological transition from fibroblast-like preadipocyte to lipid-laden mature adipocyte requires extensive rearrangement of the cytoskeletal network, the lack of actin cytoskeleton remodelling, as seen in the cells deficient of seipin, 14-3-3β or cofilin-1, may account for the observed defects in lipid accumulation and adipogenic transformation. Collectively, these data support that cofilin-1 is essential for adipocyte development, possibly through its ability to sever F-actin and remodel the cytoskeleton.

Defective adipocyte development in cells expressing cofilin-1-severing-resistant actin

To further test whether cofilin-1-mediated actin remodelling contributes to the regulation of adipogenesis, we generated stable 3T3-L1 cell lines expressing EGFP-fused wild-type β-actin (EGFP-Actin-WT) or cofilin-1 severing-resistant actin mutant (EGFP-Actin-D11N) (13), and examined lipid accumulation and total lipid content after differentiation. EGFP-Actin-WT and EGFP-Actin-D11N were expressed at comparable levels (Supplementary Material, Fig. S7A) and incorporated into the actin filament, indistinguishable from endogenous actin (Fig. 7A). Prior to differentiation, both cell lines exhibited clear and intact actin fibre networks (Fig. 7A and Supplementary Material, Fig. S7B). After adipogenic induction, the cells expressing EGFP-Actin-WT displayed diffuse EGFP-actin staining and clear cortical actin structure, consistent with dramatic F-actin depolymerization. In contrast, the cells expression EGFP-Actin-D11N retained relatively intact actin fibres, suggesting that actin resistant to cofilin-1-mediated-severing delays overall actin cytoskeleton remodelling (Supplementary Material, Fig. S7B). Moreover, compared with

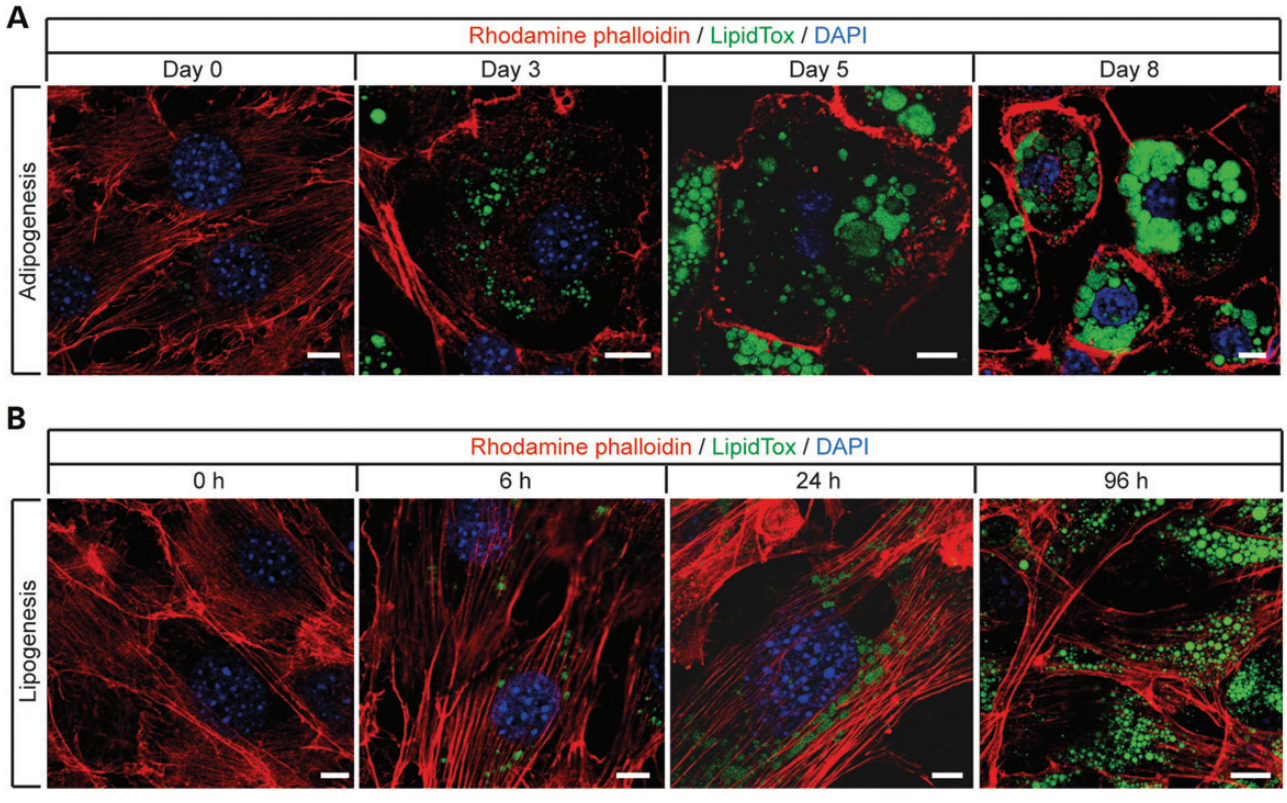

Figure 4. Actin cytoskeleton undergoes active remodelling during adipogenesis but not lipogenesis. (**A**) 3T3-L1 cells at Days 0, 3, 5 and 8 after adipogenic cocktail treatment were fixed, co-stained with rhodamine phalloidin (red) and LipidTOX (green), and imaged on a confocal microscope for visualizing actin filaments and LDs, respectively. Scale bars = 10 μm. (**B**) For visualization of LD production under OA treatment, 3T3-L1 cells were treated with 400 μM OA complexed to 0.5% BSA for different time points (0, 6, 24 and 96 h) prior to fixation with 4% formaldehyde. Actin network and LDs were stained with rhodamine phalloidin (red) and LipidTOX (green), respectively, and visualized under a confocal microscope. Scale bars = 10 μm.

EGFP-Actin-WT cells, EGFP-Actin-D11N cells exhibited dramatically reduced lipid accumulation (Fig. 7B) and total lipid content (Fig. 7C), indicating that defective cytoskeletal remodelling due to the expression of severing-resistant actin impairs lipid storage during adipogenesis. These results suggest that cofilin-1-mediated actin cytoskeleton remodelling may be a prerequisite step for adipocyte formation.

DISCUSSION

Preadipocytes must undergo both significant transcriptional reprogramming and morphological cytoskeleton remodelling to become mature adipocytes (14). The Berardinelli–Seip congenital lipodystrophy gene *BSCL2* was previously identified as an important regulator in adipocyte development. However, it has not been clear how its encoding ER-resident protein contributes to adipocyte development. Our previous study has demonstrated that seipin regulates lipid homeostasis by preventing lipids from overloading in non-adipocytes while promoting lipid storage in adipocytes (4). In this report, we extend those findings by identifying 14-3-3β as a binding partner to seipin's cytosolic N- and C-termini. Our data favor a model in which 14-3-3β transduces a seipin-guided lipid storage signal to the cytoplasm, directing cofilin-1-mediated cytoskeletion reorganization, thereby enabling the remodelling process that is necessary for preadipocytes to become mature adipocytes (Fig. 7D). The rearrangement of actin networks from stress fibres to cortical actin may be beneficial for adipocyte function since membrane reorganization is actively mediated by dynamic cortical actin (15). A large body of work has demonstrated that glucose uptake is dependent on the dynamics of cortical actin in adipocytes (16–18), which is necessary for efficient uptake of additional nutrients. Our model suggests that during adipogenesis, excess nutrients stimulate the uptake of lipids into preadipocytes, and the accumulation of lipids in the ER is sensed by seipin. This energy storage signal is transduced to the cytoplasm where 14-3-3β mediates the recruitment of cofilin-1, thereby coordinating the remodelling of actin cytoskeleton for adipocyte formation. This model suggests two beneficial consequences for energy storage downstream of actin cytoskeleton remodelling: cortical actin organization for glucose transport and nutrient uptake, and accommodation of LD expansion through dynamic dissolution of stress fibres.

Congenital generalized lipodystrophy type 2 (BSCL2) is the most severe type of lipodystrophy with near complete loss of both mechanical and metabolic adipose tissue. Characterization of this disease may elucidate key molecular events in the process of adipocyte differentiation, which may be helpful in the development of effective therapeutics against obesity and insulin resistance. The functional importance of *BSCL2* gene-encoding protein seipin in adipocyte development has been demonstrated with *in vitro* and *in vivo* studies (2,3,8,9). However, the precise

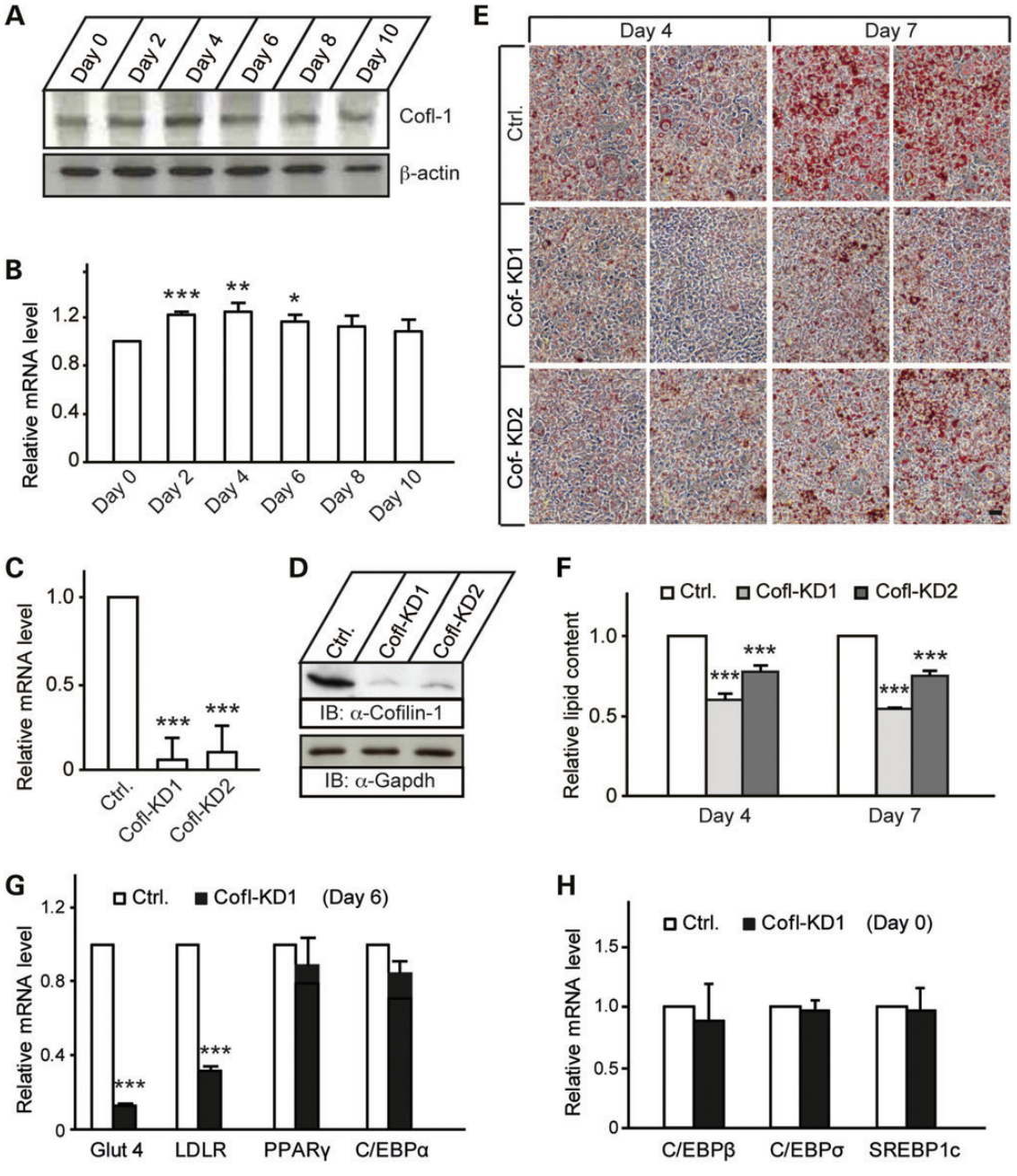

Figure 5. Knockdown of cofilin-1 inhibits adipogenesis. (**A** and **B**) Expression levels of cofilin-1 as assessed by immunoblotting (A) and qPCR (B) at various time points during adipocyte differentiation. Data are presented as mean ± SD. $N = 3$ independent experiments, each measured in triplicates. (**C** and **D**) Two stable cell lines (Cofl-KD1 and Cofl-KD2) with efficient downregulation of cofilin-1 compared with the control group (Ctrl., scrambled siRNA) were selected based on the mRNA levels by qPCR (C) or protein levels (D). (**E**) Stable cofilin-1 knockdown 3T3-L1 cells (Cofl-KD1 and Cofl-KD2) were stained with oil-red O at Days 4 and 7 after adipogenic cocktail treatment and assessed by microscopy (20×). Two representative fields per group are shown. Scale bars = 50 μm. (**F**) Isopropanol extracts of oil-red O were used to assess the relative total lipid content in cofilin-1 KD cells at Days 4 and 7 post adipogenic cocktail treatment. Data are presented as mean ± SD. $N = 3$–4 independent experiments. (**G**) Expression levels of adipocyte markers, GLUT4, LDLR and two master adipogenic regulators, PPARγ and C/EBPα, were determined by qPCR in stable KD cells (Cofl-KD) in comparison with the control group (Ctrl., scrambled siRNA) at Day 6. (**H**) Expression levels of adipogenic initiation regulators, C/EBPβ, C/EBPσ and Srebp1c, were determined by qPCR in stable KD cells in comparison with control cells (Ctrl., scrambled siRNA) at Day 0. Data are presented as mean ± SD. $N = 3$–4 independent experiments, each measured in triplicates. $^{*}P < 0.05$ and $^{**}P < 0.01$ versus control cells.

underlying mechanism is largely unknown. In our previous studies, we demonstrated that mammalian seipin contains at least two distinct functional domains, which may cooperate with each other to regulate lipid storage and control lipid homeostasis (4). Here, we propose that actin cytoskeleton remodelling is central to seipin's control of lipid homeostasis and adipogenesis.

We have identified seipin as a possible regulator of cofilin-1-mediated actin cytoskeleton remodelling, which is important for adipocyte development and maturation. It was observed that

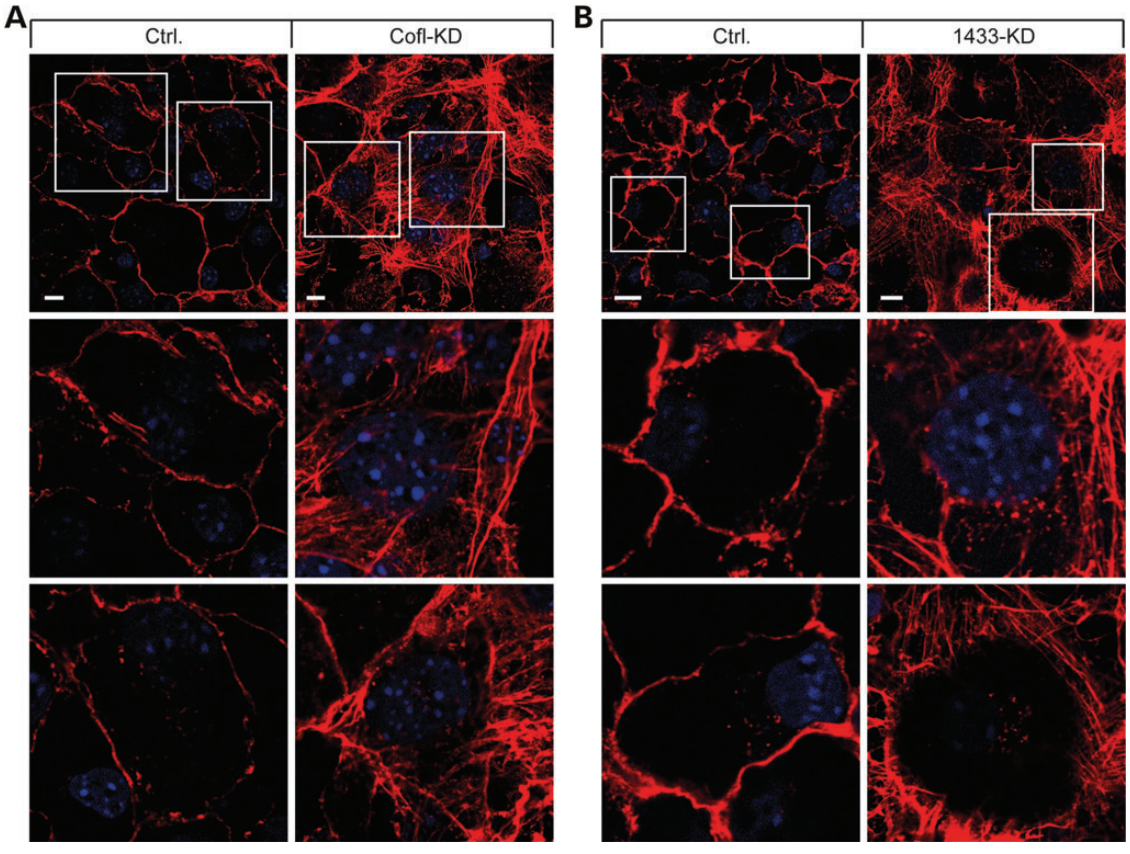

Figure 6. Resistance to actin cytoskeleton remodelling in cofilin-1 or 14-3-3β KD cells during adipogenesis. (**A**) Rhodamine-phalloidin staining of actin cytoskeleton in differented 3T3-L1 cells (Day 5). Cofilin-1 KD (Cofl-KD) cells show complex intact actin stress fibres across the cell body, whereas control cells display peripheral cortical arrangement of actin cytoskeleton. (**B**) A similar actin cytoskeleton phenotype is seen in 14-3-3β KD (1433-KD) cells. Scale bars = 10 μm.

actin cytoskeleton undergoes dramatic reorganization from stress fibres to cortical localization during adipocye differentiation. The resultant formation of cortical actin may be functionally important for adipocyte development and energy storage in adipocytes. Previous reports have shown that the organization of cell surface molecules can form transient nanoclusters that is actively and spatiotemporally regulated by cortical actin dynamics (15). As adipocytes constitute a key endocrine organ that controls energy homeostasis, it is not surprising that receptors and other membrane-associated molecules must maintain the ability to rapidly respond to environmental nutrient conditions, which may be facilitated by cortically localized actin. For example, glucose uptake in adipocytes relies on the dynamics of cortical actin to regulate Glut-4 localization (19–21). Here, we find that actin cytoskeleton remodelling is mediated by the actin-severing protein cofilin-1. RNAi-mediated KD of cofilin-1 retards actin cytoskeleton remodelling and inhibits lipid accumulation during adipogenesis. The actin remodelling defect may arrest cells at an immature state with aberrant energy storage, as only negligible LDs could be formed transiently. In larger organisms, adipocytes rely on LD for long-term energy storage, and lipid mobilization in response to nutrient availability is under tight control. Thus, adipocytes may regulate a variety of functions through remodelling of the cortical actin network.

Adipocyte differentiation has been well studied at the transcriptional level (22–25), the importance of cytoskeleton remodelling, including microtubule- and actin-based remodelling, has only been recognized recently. Generally, the initial triggering of C/EBPβ and C/EBPσ transcriptional factors results in the activation of PPARγ and C/EBPα, two master regulators of the development and maintenance of adipocytes (26,27). At the cellular level, this is characterized by LD accumulation and expansion, accompanied by a morphological transition from a fibroblast-like preadipocyte to a spherical mature adipocyte. The morphological change in adipogenic conversion is dependent on cytoskeleton remodelling. Microtubule cytoskeleton remodelling actively facilitates adipocyte development (14), and our current data suggest that actin also plays a central role. We propose that cytoskeleton remodelling is necessary for the complete reprogramming of fibroblast-like preadipocytes into mature adipocytes.

Our study indicates that 14-3-3β serves as a link between seipin-guided lipid storage and confilin-1-mediated cytoskeleton remodelling. The 14-3-3 family of scaffolding proteins is known to localize cofilin and control the dynamics of actin turnover (28). Phosphorylation of Ser24 appears to be sufficient for cofilin binding to 14-3-3, as indicated in this study and other work (29,30). Evidence suggests that phosphorylation of Ser3 on cofilin may also contribute to this binding (29). The upstream regulators LIM kinase and Slingshot phosphatase, which control

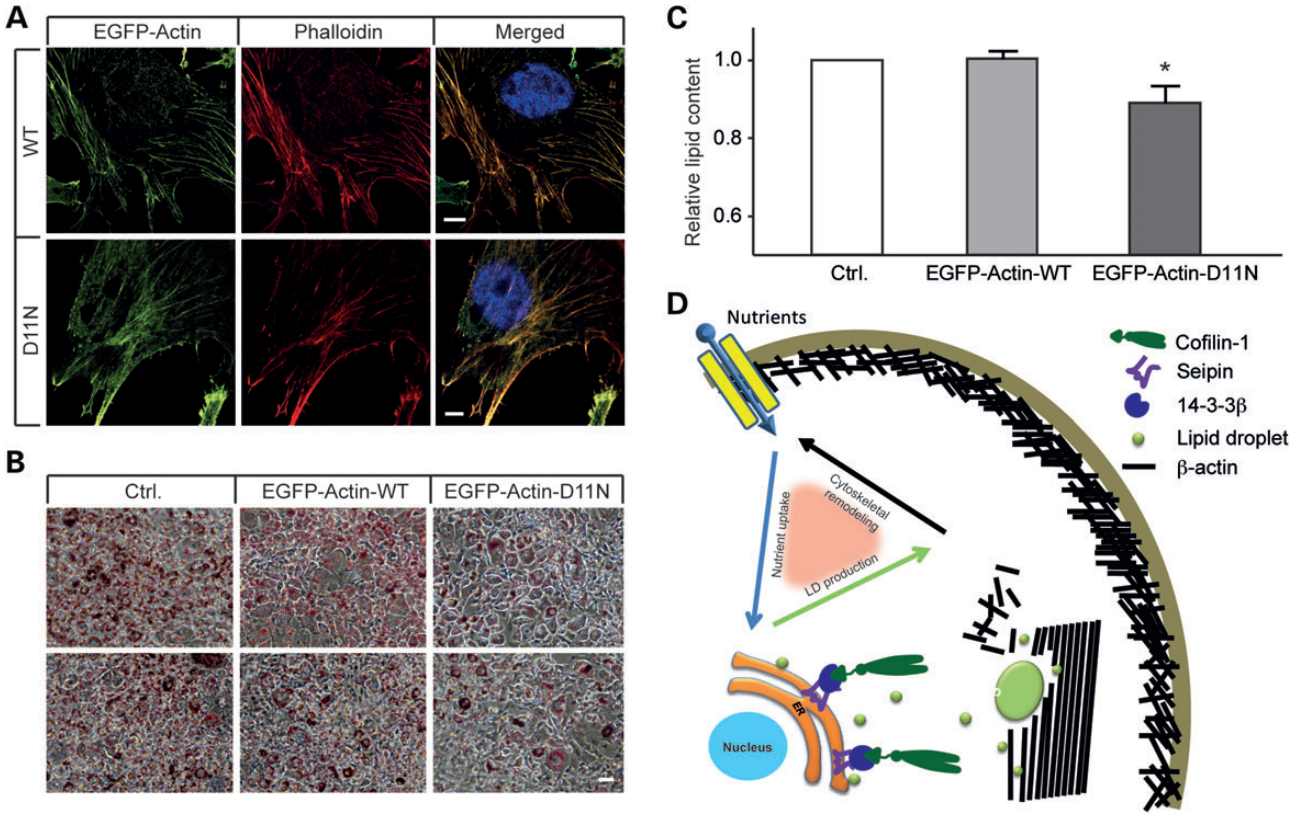

Figure 7. Delayed adipocyte development and reduced lipid accumulation in 3T3-L1 cells expressing a cofilin-1 severing resistant actin mutant. (**A**) Stable 3T3-L1 cells expressing EGFP-β-actin (EGFP-Actin-WT) or EGFP-β-actin-D11N (EGFP-Actin-D11N) were fixed, stained with rhodamine phalloidin and imaged on a confocal microscope. Note that EGFP-tagged β-actin was well incorporated into the actin filament network. Scale bars = 10 μm. (**B**) Stable 3T3-L1 cells expressing empty vector (Ctrl.), EGFP-β-actin-WT (EGFP-Actin-WT) or EGFP-β-actin-D11N (EGFP-Actin-D11N) were stained with oil-red O and assessed by microscopy (20×). Two representative fields are shown for each group. Scale bars = 100 μm. (**C**) Isopropanol extracts of oil-red O from the cells in (B) were used to determine the relative total lipid content. Data are presented as mean ± SD. $N = 3$ independent experiments. (**D**) A proposed model for the role of actin cytoskeleton remodelling in adipocyte formation. Read the text for details.

the phosphorylation status of Ser3, also interact with cofilin (31,32). Collectively, 14-3-3 may spatiotemporally localize cofilin and its regulators to coordinate the control of actin dynamics. This is supported by the colocalization of cofilin and 14-3-3 at synaptic sites, where they regulate the actin turnover for acetylcholine receptor trafficking (28). Similarly, 14-3-3β may respond to seipin-guided lipid storage signals and direct cofilin to reorganize actin cytoskeleton during adipogenesis. In this manner, 14-3-3β may serve as a platform for additional molecular processes required for adipogenesis. For example, triacylglycerol synthesis may be directly related to this process, as the cytoplasmic localization of lipin-1 is controlled by 14-3-3 in adipocytes (33).

In summary, we propose that 14-3-3β coordinates a cytoskeleton remodelling process in response to seipin-mediated lipid storage signals during adipogenesis. To our knowledge, this is the first report to provide a mechanism as to how the ER-resident protein seipin plays an essential role in adipogenesis. Our work also indicates that an active cytoskeleton remodelling during adipogenesis is necessary to accommodate LD expansion and regulate adipocyte formation. Future studies may be directed at investigating the function of seipin and cytoskeleton remodelling in adipocyte formation, which may offer new strategies to fight obesity and its associated morbidities.

MATERIALS AND METHODS

Animal welfare

Ten-week-old C57BL/6 mice were fed a standard chow diet for 8 weeks. Perigonadal adipose tissues were collected for protein extraction and immunoblotting. All experiments involving animals were reviewed and approved by the Institutional Animal Care and Use Committee of Agency for Science Technology and Research (A*STAR).

DNA plasmids

Seipin truncated constructs were a generous gift from Dr Ito (10). For knockdown of 14-3-3β and cofilin-1, targeted short hairpin RNA (shRNA) sequences were cloned into L309 vectors (Supplementary Material, Table S1). For generation of GST-fused C-terminus of seipin (GST-CSP), primers (5′-GC AGA TCT CCC CGC CAC CGC TTC TCT CT-3′ and 5′-GG GTCGAC TCA GGAACTGGAGCAGGTC-3′) were used to amplify the cytosolic C-terminus of murine *seipin*, and the resulting PCR product was cloned into a pGEX-KG vector. Plasmids containing cDNA of GST fused or Flag-tagged 14-3-3β protein were acquired from Addgene (Plasmids 13276 and 8999) (11). For site-directed mutagenesis, cDNAs encoding full-length murine

cofilin-1 in a pmCherry-C1 vector with an N-terminal fused mCherry protein was purchased from Addgene (34). Mutations of serine 24 to alanine (S24A) and glutamic acid (S24D), and aspartic acid 11 to asparagine (D11N) were introduced by site-directed mutagenesis using the QuickChange kit (Invitrogen). The DNA constructs expressing β-actin with N-terminal fused EGFP were also obtained from Addgene (35). All the corresponding coding cDNA sequences were transferred into L304 lentiviral vectors (4), and verified by sequencing.

Cell culture

The 3T3-L1 preadipocytes (ATCC) were maintained in high glucose DMEM supplemented with 10% FCS (Gibco BRL). 3T3-L1 pre-adipocytes were seeded in 24-well plates, and adipocyte differentiation was induced 2 days after cells reached confluence (Day 0) in high glucose (HG)-DMEM + 10% FBS (Gibco BRL) with an adipogenic cocktail containing 1 μM dexamethasone (Dex), 0.5 mM isobutylmethylxanthine (IBMX) and 100 nM insulin. Forty-eight hours later (Day 2), cells were switched to HG-DMEM + 10% FBS with 100 nM insulin for adipocyte differentiation. After fully differentiated (Day 8), cells were maintained in HG-DMEM + 10% FBS, which was changed every 2 days. 293TN cells (System Biosciences) were grown in HG-DMEM + 10% FBS. All cells were maintained at 37°C in a 5% CO_2 humidified incubator.

Lentivirus packaging and infection

The lentiviral shuttle vectors containing target genes and three helper plasmids (encoding HIV-1 gag-pol, HIV-1 rev and VSV-G envelope) were co-transfected into the 293TN cells according to the established procedures (4,14). Twelve to 14 h after transfection, the medium was removed and replaced with fresh medium. The medium containing the viral particles was harvested 48 h later and filtered through 0.45-μm filters. The virus-containing medium along with 8 μg/ml of polybrene (Sigma) was added to 3T3-L1 cells for overnight infection, and the medium was replaced with fresh 10% FCS/DMEM medium the following day.

Real-time quantitative PCR

Total RNA was isolated from cultured cells with TRIzol (Invitrogen) at appropriate time points and reverse transcribed using SuperScript II reverse transcriptase and random primers (Fermentas). A real-time quantitative PCR (qPCR) was performed on a StepOnePlus Real-Time PCR System (Applied Biosystems) using an SYBR Green PCR Master Mix reagent kit (Applied Biosystems). The expression level of TBP (TATA-box binding protein) was used as an internal control. The sequences for all primers used in this study are listed in Supplementary Material, Table S2.

Lipid droplet staining and visualization

To visualize LD formation by Bodipy staining, cells grown on collagen-coated coverslips were washed with PBS and incubated in DMEM containing 0.4 mM OA complexed to 0.5% bovine serum albumin (BSA) and 6 μM Bodipy FL C16 (Invitrogen) for 1, 4 or 18 h. Labelling of cells with fluorescent FA was stopped by washing cells with PBS and fixed immediately with 4% paraformaldehyde in PBS. For LipiTOX staining of LDs, 3T3-L1 cells were plated in 24-well plates with growth medium. The cells were treated with 0.4 mM OA complexed to 0.5% BSA for 18 h prior to fixation with 4% formaldehyde. LDs were stained with LipidTOX according to the manufacturer's manual and visualized under a confocal microscope (Nikon).

Oil-red O staining and isopropanol extraction

Oil-red O staining and isopropanol extraction were performed as previously described (14). The stained cells were imaged on a Nikon TS100 microscope before they were air-dried. Stained lipids were extracted using isopropanol for lipid content measurements. OD measurements of extracted solutions were taken at 500 nm wavelength to determine the relative cellular lipid content.

Immunostaining and confocal imaging

3T3-L1 cells were seeded on coverslips and fixed in 4% paraformaldehyde. The cells were then permeabilized with 0.1% Triton X-100, blocked with 10% normal goat serum and probed with antibodies diluted in the blocking buffer. Coverslips were mounted on slides in the DAPI mounting medium (Invitrogen), then imaged with A1R confocal microscopy (Nikon).

Recombinant protein

For production and purification of GST and GST-fused proteins, plasmids containing corresponding genes were transformed and expressed in BL21 bacterial cells. Isopropyl β-D-1-thiogalactopyranoside (final concentration 200 μM) was used to induce the expression of GST-fused proteins for 5 h at 37°C. The resultant GST-fusion proteins were purified using a glutathione column. Protein concentration was measured by using a DC Protein Assay (Bio-Rad). Protein purity was assessed by SDS-PAGE through coomassie blue staining.

Co-immunoprecipitation (Co-IP)

293TN cells were co-transfected with plasmids expressing Flag-tagged 14-3-3β and Myc-tagged seipin mutants (10,14). Two days after transfection, total lysates were prepared and incubated with an anti-Myc antibody for 4 h. Then, protein-A agarose beads were added, and after a 2 h incubation, unbound material was washed away with lysis buffer. Bound material was boiled in Laemmli buffer and subjected to western blot with anti-Flag antibody (Sigma). For Co-IP in 3T3-L1 adipocytes, preadipocytes were infected with viruses expressing Myc-tagged seipin, then treated with a standard cocktail to induce differentiation. Fully differentiated cells were treated with or without insulin and isoproterenol. Cell lysis, immunoprecipitation and subsequent analysis were similar to the process as described above, except that anti-cofilin-1 antibody (Abgent) was used.

Mass spectrometry

The shotgun LC MALDI TOF-TOF and Q-TOF MS/MS technique were applied to identify binding partners. For identification of binding partners to the C-terminus of seipin, adipose tissue lysate was pulled down by a GST-fused C-Seipin peptide and compared with GST peptide alone. For identification of binding partners to 14-3-3β during adipogenesis, fully differentiated 3T3-L1 cells were treated with or without insulin. Treated cells [basal (without insulin treatment) and insulin (with insulin treatment)] were lysed and pulled down by GST-14-3-3β. The eluted protein mixtures were desalted and concentrated via ultrafiltration and freeze drying, then denatured and reduced in 20 μl of 50 mM ammonium bicarbonate buffer containing 0.1% SDS and 25 mM DTT at 95°C for 5 min, and alkylated with 50 mM IAA followed by in-solution digestion with 2 μg trypsin (Promega) for 16 h at 37°C. Peptide mixtures were acidified by adjusting the concentration of 0.1% TFA or 1% FA, and injected into Agilent Q-TOF 6520 ChipLC MS/MS system with the mobile phase gradient from 0.1% FA-ACN 5% to 95% within 60 min or Dionex Ultimate 3000 Nano LC with Acclaim® PepMap100 C18 column (ID 300 μm × 15 cm, 3 μm, 100 Å) coupled with Bruker proteineer fc, with the mobile phase gradient from 0.1% TFA-ACN 5% to 90% within 60 min. MALDI-TOF-TOF MS/MS was carried out at Bruker Ultraflex III TOF-TOF with support of the software FlexControl 3.0, WarpLC1.2, FlexAnalysis 3.0 and Biotools 3.2. The Agilent 6520 ESI Q-TOF MS data file (.d) was converted to mzdata.xml by MassHunter, and submitted to in-house MatrixScience mascot server 2.4 in ms/ms ion search program against the Uniprot mouse database.

Western blot analysis

Adipose tissue samples or cultured cells were homogenized in a Tris-based lysis buffer on ice. Protein concentrations of the resultant lysates were quantified using the DC Protein assay (Bio-Rad Laboratories). Samples containing 50 μg of protein were loaded into each well, resolved on a polyacrylamide gel and blotted on to a nitrocellulose membrane using iBlot (Invitrogen). Membranes were then probed with antibodies and visualized with ECL or ECLPlus reagents (GE Healthcare Life Sciences). Antibodies used in the present study were: anti-14-3-3β (Abgent, dilution 1:1000), anti-Flag (Sigma, dilution 1:2000), anti-Myc (Santa Cruz, dilution 1:2000), anti-cofilin-1 (Cell Signalling, dilution 1:1000), anti-Gapdh (Santa Cruze, dilution 1: 3000) and anti-β-actin (Santa Cruz, dilution 1:5000).

Statistical analysis

Comparisons of data were made by using two-tailed unpaired *t*-test with equal variance. Statistical significance limit was displayed as $^{*}P < 0.05$, $^{**}P < 0.01$ or $^{***}P < 0.001$ or as indicated in figures.

SUPPLEMENTARY MATERIAL

Supplementary Material is available at *HMG* online.

ACKNOWLEDGEMENTS

We thank the SBIC-Nikon Imaging Center for support on microscopy.

Conflict of Interest statement. None declared.

FUNDING

This study was supported by intramural funding from A*STAR Biomedical Research Council (W.H.).

REFERENCES

1. Magre, J., Delepine, M., Khallouf, E., Gedde-Dahl, T. Jr, Van Maldergem, L., Sobel, E., Papp, J., Meier, M., Megarbane, A., Bachy, A. *et al.* (2001) Identification of the gene altered in Berardinelli–Seip congenital lipodystrophy on chromosome 11q13. *Nat. Genet.*, **28**, 365–370.
2. Chen, W., Chang, B., Saha, P., Hartig, S.M., Li, L., Reddy, V.T., Yang, Y., Yechoor, V., Mancini, M.A. and Chan, L. (2012) Berardinelli–Seip congenital lipodystrophy 2/seipin is a cell-autonomous regulator of lipolysis essential for adipocyte differentiation. *Mol. Cell Biol.*, **32**, 1099–1111.
3. Cui, X., Wang, Y., Tang, Y., Liu, Y., Zhao, L., Deng, J., Xu, G., Peng, X., Ju, S., Liu, G. *et al.* (2011) Seipin ablation in mice results in severe generalized lipodystrophy. *Hum. Mol. Genet.*, **20**, 3022–3030.
4. Yang, W., Thein, S., Guo, X., Xu, F., Venkatesh, B., Sugii, S., Radda, G.K. and Han, W. (2013) Seipin differentially regulates lipogenesis and adipogenesis through a conserved core sequence and an evolutionarily acquired C-terminus. *Biochem. J.*, **452**, 37–44.
5. Lundin, C., Nordstrom, R., Wagner, K., Windpassinger, C., Andersson, H., von Heijne, G. and Nilsson, I. (2006) Membrane topology of the human seipin protein. *FEBS Lett.*, **580**, 2281–2284.
6. Ebihara, K., Kusakabe, T., Masuzaki, H., Kobayashi, N., Tanaka, T., Chusho, H., Miyanaga, F., Miyazawa, T., Hayashi, T., Hosoda, K. *et al.* (2004) Gene and phenotype analysis of congenital generalized lipodystrophy in Japanese: a novel homozygous nonsense mutation in seipin gene. *J. Clin. Endocrinol. Metab.*, **89**, 2360–2364.
7. Miranda, D.M., Wajchenberg, B.L., Calsolari, M.R., Aguiar, M.J., Silva, J.M., Ribeiro, M.G., Fonseca, C., Amaral, D., Boson, W.L., Resende, B.A. *et al.* (2009) Novel mutations of the BSCL2 and AGPAT2 genes in 10 families with Berardinelli-Seip congenital generalized lipodystrophy syndrome. *Clin. Endocrinol. (Oxf.)*, **71**, 512–517.
8. Chen, W., Yechoor, V.K., Chang, B.H., Li, M.V., March, K.L. and Chan, L. (2009) The human lipodystrophy gene product Berardinelli–Seip congenital lipodystrophy 2/seipin plays a key role in adipocyte differentiation. *Endocrinology*, **150**, 4552–4561.
9. Payne, V.A., Grimsey, N., Tuthill, A., Virtue, S., Gray, S.L., Dalla Nora, E., Semple, R.K., O'Rahilly, S. and Rochford, J.J. (2008) The human lipodystrophy gene BSCL2/seipin may be essential for normal adipocyte differentiation. *Diabetes*, **57**, 2055–2060.
10. Ito, D., Fujisawa, T., Iida, H. and Suzuki, N. (2008) Characterization of seipin/BSCL2, a protein associated with spastic paraplegia 17. *Neurobiol. Dis.*, **31**, 266–277.
11. Yaffe, M.B., Rittinger, K., Volinia, S., Caron, P.R., Aitken, A., Leffers, H., Gamblin, S.J., Smerdon, S.J. and Cantley, L.C. (1997) The structural basis for 14-3-3:phosphopeptide binding specificity. *Cell*, **91**, 961–971.
12. Feng, T., Szabo, E., Dziak, E. and Opas, M. (2010) Cytoskeletal disassembly and cell rounding promotes adipogenesis from ES cells. *Stem Cell Rev.*, **6**, 74–85.
13. Umeki, N., Nakajima, J., Noguchi, T.Q., Tokuraku, K., Nagasaki, A., Ito, K., Hirose, K. and Uyeda, T.Q. (2013) Rapid nucleotide exchange renders Asp-11 mutant actins resistant to depolymerizing activity of cofilin, leading to dominant toxicity in vivo. *J. Biol. Chem.*, **288**, 1739–1749.
14. Yang, W., Guo, X., Thein, S., Xu, F., Sugii, S., Baas, P.W., Radda, G.K. and Han, W. (2013) Regulation of adipogenesis by cytoskeleton remodelling is facilitated by acetyltransferase MEC-17-dependent acetylation of alpha-tubulin. *Biochem. J.*, **449**, 605–612.
15. Gowrishankar, K., Ghosh, S., Saha, S., C, R., Mayor, S. and Rao, M. (2012) Active remodeling of cortical actin regulates spatiotemporal organization of cell surface molecules. *Cell*, **149**, 1353–1367.

16. Kanzaki, M. and Pessin, J.E. (2001) Insulin-stimulated GLUT4 translocation in adipocytes is dependent upon cortical actin remodeling. *J. Biol. Chem.*, **276**, 42436–42444.
17. Bose, A., Guilherme, A., Robida, S.I., Nicoloro, S.M., Zhou, Q.L., Jiang, Z.Y., Pomerleau, D.P. and Czech, M.P. (2002) Glucose transporter recycling in response to insulin is facilitated by myosin Myo1c. *Nature*, **420**, 821–824.
18. Saltiel, A.R. and Kahn, C.R. (2001) Insulin signalling and the regulation of glucose and lipid metabolism. *Nature*, **414**, 799–806.
19. Lopez, J.A., Burchfield, J.G., Blair, D.H., Mele, K., Ng, Y., Vallotton, P., James, D.E. and Hughes, W.E. (2009) Identification of a distal GLUT4 trafficking event controlled by actin polymerization. *Mol. Biol. Cell*, **20**, 3918–3929.
20. Omata, W., Shibata, H., Li, L., Takata, K. and Kojima, I. (2000) Actin filaments play a critical role in insulin-induced exocytotic recruitment but not in endocytosis of GLUT4 in isolated rat adipocytes. *Biochem. J.*, **346** Pt 2, 321–328.
21. Brozinick, J.T. Jr, Berkemeier, B.A. and Elmendorf, J.S. (2007) "Actin"g on GLUT4: membrane & cytoskeletal components of insulin action. *Curr. Diabetes Rev.*, **3**, 111–122.
22. Cristancho, A.G. and Lazar, M.A. (2011) Forming functional fat: a growing understanding of adipocyte differentiation. *Nat. Rev. Mol. Cell Biol.*, **12**, 722–734.
23. Hansen, J.B. and Kristiansen, K. (2006) Regulatory circuits controlling white versus brown adipocyte differentiation. *Biochem. J.*, **398**, 153–168.
24. Morrison, R.F. and Farmer, S.R. (1999) Insights into the transcriptional control of adipocyte differentiation. *J. Cell Biochem.*, Suppl. **32–33**, 59–67.
25. Rosen, E.D. and MacDougald, O.A. (2006) Adipocyte differentiation from the inside out. *Nat. Rev. Mol. Cell Biol.*, **7**, 885–896.
26. Siersbaek, R., Nielsen, R. and Mandrup, S. (2012) Transcriptional networks and chromatin remodeling controlling adipogenesis. *Trends Endocrinol. Metab.*, **23**, 56–64.
27. Fajas, L., Fruchart, J.C. and Auwerx, J. (1998) Transcriptional control of adipogenesis. *Curr. Opin. Cell Biol.*, **10**, 165–173.
28. Lee, C.W., Han, J., Bamburg, J.R., Han, L., Lynn, R. and Zheng, J.Q. (2009) Regulation of acetylcholine receptor clustering by ADF/cofilin-directed vesicular trafficking. *Nat. Neurosci.*, **12**, 848–856.
29. Gohla, A. and Bokoch, G.M. (2002) 14-3-3 Regulates actin dynamics by stabilizing phosphorylated cofilin. *Curr. Biol.*, **12**, 1704–1710.
30. Sakuma, M., Shirai, Y., Yoshino, K., Kuramasu, M., Nakamura, T., Yanagita, T., Mizuno, K., Hide, I., Nakata, Y. and Saito, N. (2012) Novel PKCalpha-mediated phosphorylation site(s) on cofilin and their potential role in terminating histamine release. *Mol. Biol. Cell*, **23**, 3707–3721.
31. Birkenfeld, J., Betz, H. and Roth, D. (2003) Identification of cofilin and LIM-domain-containing protein kinase 1 as novel interaction partners of 14-3-3 zeta. *Biochem. J.*, **369**, 45–54.
32. Soosairajah, J., Maiti, S., Wiggan, O., Sarmiere, P., Moussi, N., Sarcevic, B., Sampath, R., Bamburg, J.R. and Bernard, O. (2005) Interplay between components of a novel LIM kinase-slingshot phosphatase complex regulates cofilin. *EMBO J.*, **24**, 473–486.
33. Peterfy, M., Harris, T.E., Fujita, N. and Reue, K. (2010) Insulin-stimulated interaction with 14-3-3 promotes cytoplasmic localization of lipin-1 in adipocytes. *J. Biol. Chem.*, **285**, 3857–3864.
34. Taylor, M.J., Perrais, D. and Merrifield, C.J. (2011) A high precision survey of the molecular dynamics of mammalian clathrin-mediated endocytosis. *PLoS Biol.*, **9**, e1000604.
35. Watanabe, N. and Mitchison, T.J. (2002) Single-molecule speckle analysis of actin filament turnover in lamellipodia. *Science*, **295**, 1083–1086.